The Structure - Antituberculosis Activity Relationships Study in a Series of 5-(4-Aminophenyl)-4-Substituted-2,4-Dihydro-3h-1,2,4-Triazole-3-Thione Derivatives. A Combined Electronic-Topological and Neural Networks Approach

Fatma Kandemirli[1], Nathali Shvets[2], Seda Ünsalan[3], Ilkay Küçükgüzel[3], Sevim Rollas[3], Vasyl Kovalishyn[4], Anatholy Dimoglo[2,5,*]

[1]*Department of Chemisry, Kocaeli University, Kocaeli, 41100, Turkey;* [2]*Gebze Institute of Technology, PK-141, Gebze/Kocaeli, 41400, Turkey;* [3]*Department of Pharmaceutical Chemistry, Marmara University, Faculty of Pharmacy, Haydarpasa 34668 _stanbul, Turkey;* [4]*Biomedical Department, Institute of Bioorganic Chemistry & Petrochemistry, Kyiv,02660, Ukraine*; [5]*Department of Quantum Chemistry, Institute of Chemistry, Kishinev, 2028, Moldova*

Abstract: Antituberculosis activity of several 5-(4-aminophenyl)-4-alkyl/aryl-2,4-dihydro-3H-1,2,4-triazole-3-thiones (1-9) and their thiourea derivatives (10-31) were screened for their antimycobacterial activities against *Mycobacterium tuberculosis* H37Rv using the BACTEC 460 radiometric system. Of the synthesized compounds, 10-12, 30 were the most active derivatives exhibiting more than 90 % inhibition of mycobacterial growth at 12.5 μg/mL. Structure-activity relationships study was performed for the given series by using the Electronic-Topological Method combined with Neural Networks (ETM-NN). A system of prognosis was developed as the result of training associative neural network (ASNN) using weights of pharmacophoric fragments as descriptors. Descriptors were calculated by the projection of ETM compound and pharmacophoric fragments on the elements of Kohonen's self-organizing maps (SOM). From the detailed analysis of all compounds under study, the necessary requirements for a compound to possess antituberculosis activity were formulated. The analysis have shown that any requirements violation for a molecule implies a considerable decrease or even complete loss of its activity.

Key Words: Antituberculosis activity, structure-activity relationships, electronic-topological method, neural networks.

INTRODUCTION

Worldwide, tuberculosis (TB) is a contagious disease with high mortality [1]. The rising prevalence of TB infections threatens world population. Today, it is estimated that approximately one-third of the world's population is presently infected with TB, whilst eight million new cases appear every year [2]. The treatment of TB disease always required the combined use of conventional antimycobacterial agents. Although TB is a curable disease, the treatment becomes complicated due to multi-drug administration, giving rise to side effects, exploding medication costs, and mostly results in the appearance of multi-drug resistant tuberculosis (MDRTB) [3]. On the other hand, TB often targets immunosupressed individuals and it is one of the main reasons of deaths in HIV-infected patients [4]. Hence, there is an increased demand to develop new antituberculosis agents effective against pathogens resistant to current treatment. Unlike most antibacterial agents, the mechanisms of action for several TB drugs are still not fully clarified. A number of macromolecular targets such as cell wall biosynthesis, the *M. tuberculosis* genome and other biosynthetic pathways are being delineated for the discovery of new, more effective and selective anti-TB agents. Antibacterial and antituberculosis activity of compounds possessing 1,2,4-triazole ring have been reported in numerous studies [4-8]. In the course of screening new compounds with antimycobacterial activity, we formerly synthesized several 1,2,4-triazoles, which inhibit *in vitro* growth of *Mycobacterium tuberculosis* H37Rv in varying degrees. The aim of the present study is to investigate structure-activity relationships of these compounds to better understand structural requirements of 3,4,5-trisubstituted-1,2,4-triazole derivatives for antituberculosis activity and to identify a lead compound for future work.

The goal of the present study is the search of the more potent anti-tuberculosis agents by applying the combination of a specific electronic-topological method (ETM) and neural networks (ETM-NNs) [9]. Both of them have already been successfully applied, but separately, to a wide enough variety of tasks related to the structure-activity relationships (SAR) investigation [10-18].

Previously, two novel series of 2,5-disubstituted-1,3,4-thiadiazoles and 5-aryl-2-thio-1,3,4-oxadiazoles were synthesized, their compounds structures elucidated and screened for antituberculosis activity against *Mycobacterium tuberculosis* H37Rv. With the help of the ETM-NN, Structure-Antituberculosis Activity Relationships were studied for all these compounds [19, 20]. As the result of that study, the system for the activity prediction was developed, which

*Address correspondence to this author at the Gebze Institute of Technology, PK-141, Gebze/Kocaeli, 41400, Turkey; Tel: +90 262 605 16 67; Fax: +90 262 653 84 90; E-mail: dimoglo@gyte.edu.tr

1573-4064/06 $50.00+.00

included pharmacophores, anti-pharmacophores, and conditions necessary for the activity demonstration by a compound, as well. This system is capable of identifying active compounds with high enough probability.

This work extends the study of thiadiazole derivatives with antituberculosis activity by applying a new combined approach based on the further analysis of the ETM results by means of Artificial Neural Networks (ANNs). The latter are

Table 1. Structures and Antimycobacterial Screening Results of Compounds 1-31[a].

Compound number	R_1	R_2	R_3	MIC [b] (μg/mL)	Inhibition[c] (%)	Exp	Theor
1	H	-	-	>12.5	0	–	–
2	CH_3	-	-	>12.5	8	+	– +
3	C_2H_5	-	-	>12.5	0	–	–
4	C_3H_7	-	-	>12.5	0	–	–
5	$CH_2CH=CH_2$	-	-	>12.5	0	–	–
6*	C_4H_9	-	-	>12.5	0	–	–
7	$CH_2CH_2C_6H_5$	-	-	>12.5	0	–	–
8	C_6H_{11}	-	-	>12.5	0	–	– +
9	C_6H_5	-	-	>12.5	0	–	–
10	CH_3	CH_3	-	<12.5	93	+	–
11*	CH_3	CH_2CH_3	-	<12.5	90	+	+
12	CH_3	$CH_2CH=CH_2$	-	<12.5	94	+	+
13	CH_3	C_6H_{11}	-	>12.5	10	+	+
14	CH_3	C_6H_5	-	>12.5	29	+	+
15	CH_2CH_3	$CH_2CH=CH_2$	-	>12.5	89	+	+
16*	CH_2CH_3	C_6H_{11}	-	>12.5	10	+	+
17	$CH_2CH=CH_2$	CH_3	-	>12.5	0	–	–
18	$CH_2CH=CH_2$	$CH_2CH=CH_2$	-	>12.5	71	+	+
19	$CH_2CH=CH_2$	C_6H_5	-	>12.5	0	–	–
20	C_6H_{11}	$CH_2CH=CH_2$	-	>12.5	35	+	+
21*	C_6H_{11}	C_6H_{11}	-	>12.5	12	+	–
22	$CH_2CH_2C_6H_5$	$CH_2CH=CH_2$	-	>12.5	6	+	+
23	C_6H_5	CH_3	-	>12.5	27	+	+
24	C_6H_5	CH_2CH_3	-	>12.5	17	+	–
25	C_6H_5	$CH_2CH=CH_2$	-	>12.5	12	+	+
26*	C_6H_5	C_6H_{11}	-	>12.5	13	+	+
27	C_6H_5	C_6H_5	-	>12.5	13	+	+
28	C_6H_5	$C_6H_4Cl(4)$	-	>12.5	11	+	+
29	CH_3	CH_3	H	>12.5	85	+	+
30	CH_3	$CH_2CH=CH_2$	Cl	<12.5	94	+	+
31*	C_6H_5	$CH_2CH=CH_2$	Cl	>12.5	63	+	+

[a] The data on antituberculosis activity of **10-31** are taken from our previous study [19].

[b] MIC effecting *M.tuberculosis H37Rv* ; MIC of Rifampicin = 0.25 μg/mL

[c] Reduction of mycobacterial growth using *M.tuberculosis H37Rv* at 12.5 μg/mL

*- tested compounds

capable of elucidating structure-activity relationships (SAR) because of their ability to take into account any non-linear dependencies among the values of different molecular characteristics.

MATERIALS AND METHODS

Chemistry and Antituberculosis Activity Screening

Table **1** contains data on the structures of all compounds in these series and their corresponding values of inhibition (%). Ethyl 4-(acetylamino)benzoate was obtained by heating benzocaine with acetic anhydride [21]. This product was then reacted with excess hydrazine hydrate to give 4-(acetylamino)benzoic acid hydrazide [21, 22].

Equimolar amounts of 4-(acetylamino)benzoic acid hydrazide with potassium thiocyanate or metyl-, ethyl-, allyl-, phenyl- and cyclohexyl isothiocyanates were refluxed in ethanol to yield 1-[4-(Acetylamino)benzoyl]-4-alkyl/arylthiosemicarbazides (**Ia-d,f,g**) according to the reported method [22, 23]. 1-[4-(Benzoylamino)benzoyl]-4alkyl/aryl thiosemicarbazide **Ie** was also obtained by the reaction of phenethyl isothiocyanate with 4-(benzoylamino)benzoic acid hydrazide as previously reported [24] (Scheme **1**).

Compounds **4** and **6** were synthesized from 2,4-dihydro-5-[4-(1-phenyl-3,5-dimethyl-4-pyrazolylazo)phenyl]-4-allyl/butyl-3H-1,2,4-triazole-3-thiones by refluxing with excess hydrazine hydrate as previously reported by Rollas (Scheme **2**) [25]. Use of hydrazine hydrate not only gave rise to azo reduction, but also allyl group was observed to be reduced to propyl group (compound **4**) without a catalyst.

3-Benzylthio-4-methyl-5-(4-aminophenyl)-4H-1,2,4-triazole **IIa**, 3-[(2,4-dichlorobenzyl) thio]-4-methyl-5-(4-aminophenyl)-4H-1,2,4-triazole **IIb** and 3-[(2,4-dichlorobenzyl) thio]-4-phenyl-5-(4-aminophenyl)-4H-1,2,4-triazole **IIc**, were obtained as previously described [26]. Final step comprised reaction of the amines **IIa-c** or **2,3,5,7-9** with various alkyl or aryl isothiocyanates, yielding the corresponding thioureas **10-31** (Scheme **1**) [19].

Although synthesis of **1-3, 5, 8, 9** was previously reported elsewhere, they were prepared in a different manner, starting from 1-[4-(Acetylamino)benzoyl]-4-alkyl/arylthiosemi carba-

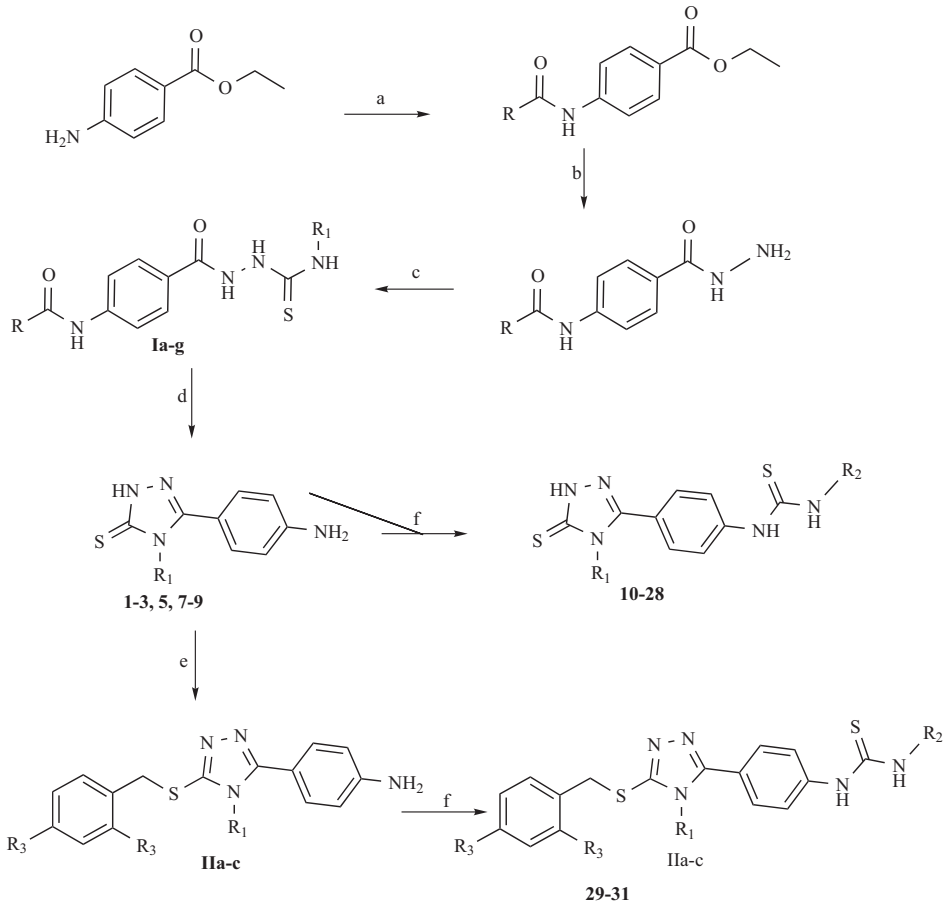

Scheme (1). Synthetic pathway for compounds **1-3, 5, 7-31**.

Key : (a) Ac_2O (reflux) or PhCOCl / Et_2O (R = Ac or Bz) ; (b) H_2N-NH_2.H_2O / EtOH, reflux; (c) R_1-NCS / EtOH, reflux ; (d) NaOH (2N), reflux ; (e) Ar-CH_2Cl / NaOH-EtOH; (f) R_2-NCS / dioxane-MeOH (2:1, v/v), reflux.

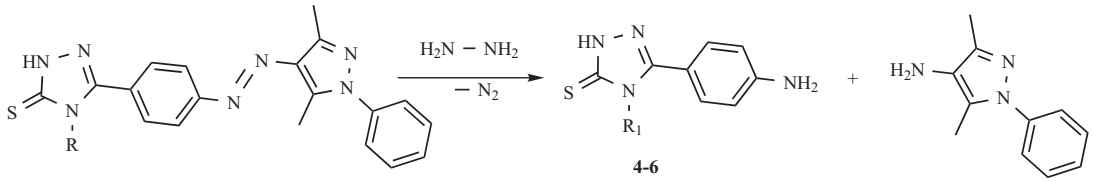

Scheme (2). Synthesis of compounds **4** and **6** *via* reductive cleavage.
(R = $-CH_2CH=CH_2$ and $-C_4H_9$; R' = $-C_3H_7$ and $-C_4H_9$ for compounds **4** and **6**, respectively).

zides (**Ia-d,f,g**) which gave the desired 1,2,4-triazoles in higher yields compared to literature method [27]. The identity and purity of the synthesized compounds were confirmed by melting points and TLC comparisons using standards of **1-3,5,7-9** obtained from 1-[4-(acetyl/benzoylamino) benzoyl]-4-alkyl/arylthiosemicarbazides [27, 28].

Compounds **1-31** were tested for the *in vitro* antituberculosis activity against *Mycobacterium tuberculosis H37Rv* on the BACTEC 12B medium using a broth microdilution assay, the Microplate Alamar Blue Assay (MABA) [29, 30]. Rifampicin was used as the standard in the antimycobacterial assays. Primary screening was performed at 6.25 mg/ml. Of these compounds, the ones which exhibited <90% inhibition in the primary screening (MIC>12.5 μg/mL) were not considered for further evaluation. More detailed information on the antituberculosis activity data for compounds **10-31** can be found in our previous work [19]. Results obtained from antituberculosis activity screening is shown in Table **1**. As shown in Table **1**, compounds **1, 3-9, 17** and **19** were completely inactive against *M.tuberculosis H37Rv* at 12.5 μg/mL, whereas remaining compounds exhibited varying degrees of inhibition (82-94%) in the primary screen. Most active derivatives were compounds **10-12** and **30** exhibiting 90-94 % inhibition against *M. tuberculosis H37 Rv*.

The Scheme of the Combined ETM-NNs Approach

Since details of the ETM can be found in literature [10, 13], we only give here the most distinguished properties of the ETM relative to other methods used in diverse SAR studies.

The main steps of the ETM-study are as follows:

1. For all compounds, calculate spatial and electron characteristics for atoms and bonds.
2. For every molecular structure being a full 3D molecular graph, form the corresponding matrix (electron-topologic matrix of contiguity, or ETMC) by choosing fixed characteristics for atoms and bonds from the data calculated.
3. Set some desirable level for the activity prediction and some precision values to have ability to compare the values of corresponding atomic and bond characteristics for any two matrices.
4. By comparing, one by one, all ETMCs with the ETMC for the most active compound, select those structural fragments $\mathbf{S_i}$ (i∈ I) that are common for all active compounds only.
5. Estimate the pharmacophoric fragments selected ("activity features") in accordance with probabilistic criterion ($\mathbf{P_a}$) and choose those that correspond to the desired level of prediction that has been set before calculations. If the fragments found are not informative enough, change some initial settings (or all of them) and repeat steps 3-5.

The combined algorithm that analyses data resulting from the ETM calculations (ETM-data) is developed on the base of Volume Learning Algorithm created previously for the analysis of CoMFA data [31]. This method is implemented as a recurrent iterative application of the Kohonen SOMs and ASNNs. The general block-schema of the ETM-NNs data analysis is presented in Fig. (**1**).

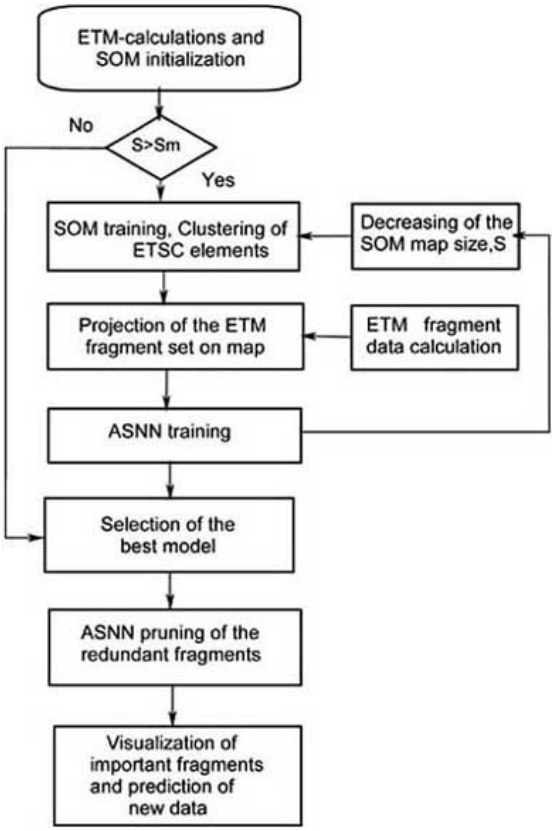

Fig. (1). Block-scheme of the ETM-NN calculations.

According to this algorithm, the process of the ETM-data further analysis is as follows:

(1) Form the initial set of input data.

(2) Initialize the Kohonen's network parameters; calculate clusters from an ETMC, for each molecule. The initial size of Kohonen's maps was $S=2*S_{ETM}$, with S_{ETM} being the size of the largest ETM matrix.

(3) Calculate the ETMC fragments. For each fragment, calculate its projection on the units of the Kohonen's SOM. Calculate the projection error (*Eq*). Calculate the weight of each fragment (1/*Eq*) and create new data set by using calculated fragment weights as parameters.

(4) Analyze ETM fragment data using ASNNs; calculate the average prediction error (*Ec*).

(5) Compare the *Ec* value to that one in the preceding stage of learning, *Ep* (initially, *Ep* = 10e-3). If *Ec* < *Ep*, the current projection of the ETM fragments is saved.

(6) Decrease the size of the Kohonen's map.

(7) Repeat steps 2 – 6 until the map size, *S*, decreases to Smin, where Smin equals to eight nodes.

(8) Select the best ETM fragments' projection, relative to the minimal value of *E*, and predict the activity of new compounds.

(9) Select the most informative ETMC fragments (after the ASNN training) by using special pruning methods.

(10) Predict activities of new compounds.

The principal idea of this approach is to determine the weights of fragments represented by submatrices of ETMCs that have been obtained from the ETM calculations. The self-organizing map is a neural network algorithm based on unsupervised learning. Training a SOM consisted of two phases [32]. The first phase, of 100,000 iterations, was used to approximately order the weight vectors of the map neurons. During the second phase, of 50,000 iterations, the values of the weight vectors were fine-tuned. The initial learning rate and neighborhood radius of the SOM were selected to be $\alpha_1=0.6$, $\sigma_1=2/5(x*y)^{0.5}$ and $\alpha_2=0.15$, $\sigma_2=2/5\sigma_1$ for the first and the second phase, respectively, where x * y corresponds to the size of the SOM map.

The supervised learning was performed using a variant of feed forward neural networks (FFNNs) trained with the back propagation algorithm known as the Associative Neural Network (ASNN) [33, 34]. The architecture of the ASNN consists of three layers, with five neurons in one hidden layer. Two output nodes were used to code class activities of compounds. Hundreds of independent networks were trained to analyze each set of variables [33].

It has been shown that pruning algorithms [35, 36] may be used to optimize the number of input parameters for FFNN learning and to select the most significant ones. These algorithms operate in a manner similar to step-wise multiple regression analysis and remove on each step by one input descriptors that was estimated to be as redundant. The pruning algorithms were used in the current study to determine significant ETM fragments of input data points of the analyzed molecules as described before [35, 36].

RESULTS AND DISCUSSION

The Search for Pharmacophores and Anti-Pharmacophores by Using ETM-NN

Conformational analysis for all compounds was done by means of a molecular mechanics method (MMX) [37]. Their electronic structures were calculated from the semi-empirical AM1 method [38].

As known, the better is the description of molecules in terms of structural parameters related to the activity in view, the better are results on pattern recognition and separation of molecules by their activities. The ETM is capable of taking into account any individual properties of atoms and bonds, and this fact may be crucial for revealing details of interactions between a biological receptor and an active molecule. The ETM calculations take into account both structural and electronic characteristics of molecules and give, as a result, a set of pharmacophores and anti-pharmacophores (fragments of activity/inactivity).

The results of conformational analysis and quantum-chemistry calculations were used to form ETMCs for all compounds. Charges on atoms (q_i) were selected for diagonal elements; the Wiberg's indices (W_{ij}) were taken as off-diagonal elements for chemically bonded atoms; otherwise, optimized distances between corresponding two atoms (R_{ij}) were used.

After processing the ETMCs, a set of pharmacophores ('activity features') was obtained. The features formed a basis for a system capable of carrying out both computer screening and forecasting activities of new drug prototypes. Optimal values of variations allowable in the process of the matrices comparison (when testing if atoms and bonds match) were found as $\Delta_1= \pm 0.05$ for diagonal elements (q_i) and $\Delta_2= \pm 0.17$ for off-diagonal values (W_{ij} and R_{ij}). To determine the most informative activity features, the desired values of probabilistic estimations α_a and _a were set as 0.70 and 0.80, correspondingly.

The set of selected pharmacophores formed the basis of a system for the anti-tubercular activity prediction. Compounds **10** and **12** possessing the highest anti-mycobacterial activity against *Mycobacterium tuberculosis* H37Rv were taken as templates for comparison. In (Fig. **2**), a sub-matrices of the template ETMC (in short, its ETSCs**)** are given, which corresponds to some of the pharmacophores revealed (Ph1, Ph2).

The given Ph1 (Fig. **2a**) pharmacophore consists of 7 atoms located in different parts of an active molecule. Ph1 is found in 18 active and 1 inactive compounds. Probability of its realization P_a is 0.90. Hydrogen atoms H_7 and H_{20} have a positive charges q= 0.15- 0.12_. On the carbon atoms of phenyl groups ($C_9 \div C_{11}$ and C_{14}) charges are close to zero. The Ph1 is very sensitive to different replacements done in the phenyl ring. A substituent change, as well as any changes

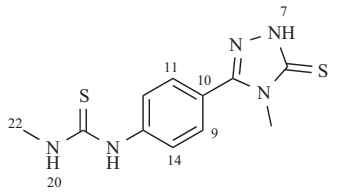

H_7	C_9	C_{10}	C_{11}	C_{14}	H_{20}	C_{22}
0.15	5.69	4.49	4.91	6.92	8.11	10.79
	0.03	1.39	2.39	1.47	4.62	7.28
		-0.01	1.38	2.45	4.54	7.36
			0.03	2.76	3.53	6.42
				-0.05	3.83	6.31
					0.12	2.91
n1/n2= 18/1;		P_α= 0.90				-0.03

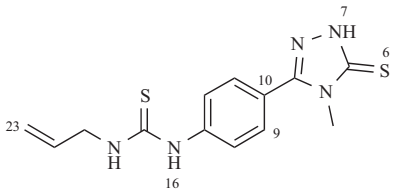

S_6	H_7	C_9	C_{10}	H_{16}	C_{23}
-0.46	2.94	5.97	5.32	9.89	13.22
	0.15	5.68	4.49	9.15	11.31
		0.03	1.43	3.94	8.28
			-0.01	4.73	8.15
n1/n2= 18/1;		P_α = 0.90		0.15	5.74
					-0.02

Fig. (2). Sub-matrices and corresponding structures of the Ph1 and Ph2 pharmacophores, obtained relative the template active compound **10** (a) and **12** (b).

in the nature of its atoms, can cause the electron density redistribution in the investigated compound.

A pharmacophore Ph2 found relative to compound **12** (template compound) is shown along with its ETSC in (Fig. **2b**). The pharmacophore Ph2 is found also in 18 active compounds and 1 inactive compound. The probability of the Ph2 realization is estimated as 0.90. The Ph2 pharmacophore contains fewer atoms than Ph1, although phenyl ring part of the molecule is present again. Sulfur atom S_6 has a high negative charge q_6= -0.46_.

The search for anti-pharmacophores has been carried out in the class of inactive molecules in the same way. In (Fig. **3**), as an example, two of the anti-pharmacophores found for the class of inactive compounds (APh1, APh2; template compounds **1** and **9**) are given.

APh1 consists of 9 atoms. As seen from Fig. **3**, atoms of the groups that break the compounds activity have not only negative, but also positive charges. Attention is to be paid to the fact that negatively charged (-0.11 ÷ -0.24_) atoms of 1,2,4-triazole ring and amine group enter these pharmacophores.

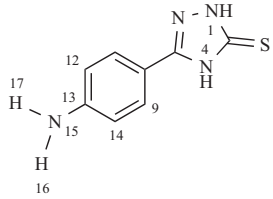

N_1	N_4	C_9	C_{12}	C_{13}	C_{14}	N_{15}	H_{16}	H_{17}
-0.11	2.15	4.69	5.75	6.46	6.00	7.82	8.41	8.25
	-0.12	3.02	4.98	5.26	4.42	6.59	6.99	7.24
		0.05	2.79	2.43	1.48	3.68	3.98	4.45
			-0.07	1.36	2.41	2.40	3.27	2.59
n2/n1= 8/1;		P_{ia}= 0.82		0.18	1.36	1.11	2.03	2.03
					-0.07	2.40	2.59	3.27
						-0.24	0.97	0.97
							0.12	1.65
								0.12

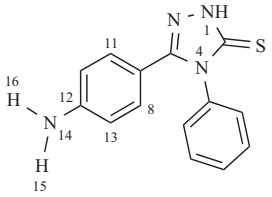

N_1	N_4	C_8	C_{11}	C_{12}	C_{13}	N_{14}	H_{15}	H_{16}
-0.07	2.17	4.75	5.66	6.43	6.04	7.78	8.40	8.22
	-0.16	3.18	5.05	5.37	4.56	6.72	7.14	7.36
		0.02	2.78	2.43	1.48	3.68	3.98	4.45
			-0.06	1.36	2.41	2.40	3.27	2.59
				0.19	1.36	1.11	2.03	2.03
n2/n1= 8/1;		P_{ia}= 0.82			-0.06	2.40	2.59	3.27
						-024	0.97	0.97
							0.12	1.65
								0.12

Fig. (3). Sub-matrices and corresponding structure of the APh1 and APh2 anti-pharmacophores, obtained relative the template inactive compounds **1** (a) and **9** (b).

As far as the order of an ETM depends on the number of atoms of the corresponding molecule, ETM data cannot be used in a straightforward manner by any method. The relationship between independent variables (elements of ETM) and dependent variable (activity) is non-linear. So, to overcome these problems, we have proposed a special algorithm being a combination of two non-linear methods.

A data set containing 31 examples was used in ETM-NN investigations. 25 of the compounds were used for the model development, and 6 randomly selected compounds (**6, 11, 16, 21, 26, 31**) were used for the model validation (see Table **1**).

The first stage of the data analysis was in finding an appropriate model by using weights of fragments as descriptors. The weights of 226 fragments (pharmacophores and anti-pharmacophores) were calculated as descriptors for each compound from their projection errors, relative to the same nodes of the Kohonen's map as in the template ETMC. Using this number of descriptors, the ASNNs recognized correctly 92%, or 22 from 25 compounds, while for the test set the result was lower, i.e. 83%, or 5 compounds from 6.

At the second stage, only four the most significant ETMC fragments were selected by the pruning methods. It should be noted, that pruning of the redundant parameters did not make the predictive ability of neural networks worse. Thus, only the activity of compound **21** from the test set and activities of compounds **8, 10, 24** from the training set (Table **1**) were predicted incorrectly.

CONCLUSION

In the course of screening new compounds with antimycobacterial activity, we formerly synthesized several 1,2,4-triazoles, which inhibit *in vitro* growth of *Mycobacterium tuberculosis* H37Rv in varying degrees. Nine of them, namely, a series of 5-(4-aminophenyl)-4-alkyl/aryl-2,4-dihydro-3H-1,2,4-triazole-3-thiones (**1-9**) and their thiourea derivatives (**10-31**), which are potential antituberculosis agents, are studied by means of the combined ETM-NN approach. The ETM calculations take into account both structural and electronic characteristics of molecules and give, as a result, a set of pharmacophores and anti-pharmacophores (fragments of activity/inactivity). A system for the activity prognostication, which is developed from the further ANNs application to the found fragments, is based on the most substantial of them and some special rules for their use.

All pharmacophores detected by the **ETM-NN** are characterized by the high enough probabilities (P_A) that lie in the limits of 0.90÷0.92 (predictive ability of the method). From the comparison of the activity features with the "breaks of activity" an explanation of why the activity varies so much in the series investigated can be seen immediately.

EXPERIMENTAL

Melting points were determined with a Büchi (B-530) apparatus and are uncorrected. Benzocaine, 4-aminobenzoic acid, ethyl and phenyl isothiocyanates were purchased from Sigma. Hydrazine hydrate was purchased from Fluka. Methyl-, allyl-, cyclohexyl isothiocyanates, acetic anhydride, benzoylchloride, sodium hydroxide, TLC plates precoated with silica-gel 60 F_{254} were obtained from Merck.

General synthesis of 5-(4-aminophenyl)-4-alkyl/aryl-2,4-dihydro-3H-1,2,4-triazole-3-thiones (1-9)

1-[4-(Acetylamino)benzoyl]-4-alkyl/arylthiosemicarbazides (**Ia-d,f,g**) (0.005 mole) were refluxed with sodium hydroxide (2N, 5 mL) for four h. Resulting sodium salts were precipitated adjusting the medium to acidic pH with diluted hydrochloric acid; washed with water, dried and recrystallized from ethanol or methanol to give compounds **1-3, 5, 8, 9**.

5-(4-Aminophenyl)-2,4-dihydro-3H-1,2,4-triazol-3-thione (1)

Prepared according to method A; m.p 282°C, yield 65 % [39].

5-(4-Aminophenyl)-4-metyl-2,4-dihydro-3H-1,2,4-triazol-3-thione (2)

Prepared according to method A ; m.p 178°C (Lit. [27] m.p. 180°C), yield 88 %.

5-(4-Aminophenyl)-4-ethyl-2,4-dihydro-3H-1,2,4-triazol-3-thione (3)

Prepared according to method A ; m.p 243°C (Lit. [27] m.p. 247°C), 73 %.

5-(4-Aminophenyl)-4-allyl-2,4-dihydro-3H-1,2,4-triazol-3-thione (5)

Prepared according to method A ; m.p 223-226°C (Lit. [27] m.p. 222-224°C), yield 92 %.

5-(4-Aminophenyl)-4-cyclohexyl-2,4-dihydro-3H-1,2,4-triazol-3-thione (8)

Prepared according to method A; m.p 249-251°C (Lit. [27] m.p. 256°C), yield 73 %.

5-(4-Aminophenyl)-4-phenyl-2,4-dihydro-3H-1,2,4-triazol-3-thione (9)

Prepared according to method A; m.p 276-279°C (Lit. [27] m.p. 282-288°C), yield 73 %.

ACKNOWLEDGMENT.

The authors thank Dr. Joseph A. Maddry from Tuberculosis Antimicrobial Acquisition and Coordinating Facility (TAACF) at the National Institute of Allergy and Infectious Disease, Southern Research Institute, GWL Hansen's Disease Center, USA, for *in vitro* evaluation of antimycobacterial activity.

REFERENCES

[1] World Health Organization, in: *Anti-tuberculosis drug resistance in the world*. The WHO/IUATLD global project on anti-tuberculosis drug resistance surveillance, **1997**.

[2] Tripathi, R.P.; Tewari, N.; Dwiwedi, N.; Tiwari, V.K. *Med. Res. Rev.,* **2005**, *25*, 93.

[3] Sriram, D.; Yogeeswari, P.; Thirumurugan, R. *Bioorg. Med. Chem. Lett.,* **2004**, *14*, 3923.
[4] Klimesova, V.; Zahajska, L.; Waisser, K.; Kaustova, J.; Möllmann, U. *Farmaco*, **2004**, *59*, 279.
[5] Mir, I.; Siddiqui, M.T. *Tetrahedron*, **1970**, *26*, 5235.
[6] Ulusoy, N.; Ergenç, N.; Ötük, G.; Kiraz, M. *Boll. Chim. Farmaceutico. Anno*., **2001**, *140*, 417.
[7] Ulusoy, N.; Gürsoy, A.; Ötük, G. *Farmaco*, **2001**, *56*, 947.
[8] Kaplancıklı, S.A.; Turan-Zitouni, G.; Chevallet, P. *J. Enzym. Inhib. Med. Chem.*, **2005**, *20*, 179.
[9] Dimoglo, A.; Kovalishyn, V.; Shvets, N.; Ahsen, V. *Mini Rev. Med. Chem*., **2005**, *5*(10), 879.
[10] Dimoglo, A.S., *Khim. Pharm. Zhur*., **1985**, *4,* 438.
[11] Bersuker I.B.; Dimoglo A.S. The Electron- Topological Approach to the QSAR Problem, In *Reviews in Computational Chemistry* (Ed. Lipkowitz, K.B. and Boyd, D.B.) VCH, New-York, **1991**; Chap.*10*. pp. 423-460.
[12] Dimoglo, A.S.; Vlad, P.F.; Shvets, N._; Coltsa, M.N. *New J. Chem*., **2001**, *25*, 283.
[13] Dimoglo, A.S.; Shvets, N.M.; Tetko, I.V.; Livingstone, D.J. *QSAR*, **2001**, *20*, 31.
[14] Dimoglo, A.S.; Chumakov, Yu.M.; Dobrova, B.N.; Shvets, N.M.; Saracoglu, M. *Arzneim. Forsch./Drug Res*., **1997**, *47*(I), 415.
[15] Dimoglo, A.S.; Sim, E.P.; Shvets, N.M.; Ahsen, V. *Mini-Rev. Med. Chem*., **2003**, *3*, 293.
[16] Manallack, D.T.; Livingstone, D. J. *Eur. J. Med. Chem*., **1999**, *34*, 195.
[17] Zupan, J.; Gasteiger, J. *Neural Networks for Chemistry and Drug Design: An Introduction*; 2nd edition, VCH: Weinheim, **1999**.
[18] Tetko, I. V.; Luik, A. I.; Poda, G. I. *J. Med. Chem.,* **1993**, *36*, 811.
[19] Küçükgüzel, I.; Küçükgüzel, _.G.; Rollas, S.; Kiraz, M. *Bioorg. Med. Chem. Lett.*, **2001**, *11*, 1703.
[20] Macaev, F.; Rusu, G.; Pogrebnoi, S.; Gudima, A.; Stingaci, E.; Vlad, L.; Shvets, N.; Kandemirli, F.; Dimoglo, A.; Reynolds, R. *Bioorg. Med. Chem.,* **2005**, *16*, 4842.
[21] Parmar, S.S.; Gupta, A. K.; Stenberg, V.I. *J. Pharm. Sci.,* **1975**, *64*, 154.
[22] Gülerman, N.; Rollas, S.; Ülgen, M.; Gorrod, J.W. *Boll. Chim. Farmaceutico Anno*., **1995**, *134*, 461.
[23] Gardner, T.S.; Smith, F.A.; Wenis, E.; Lee, J. *J. Am. Chem. Soc*., **1951**, *74*, 2106.
[24] Kalyoncuo_lu, N.; Rollas, S.; Sür-Altıner, D.; Ye_eno_lu, Y.; An_ Ö. *Pharmazie*, **1992**, *47*, 796.
[25] Rollas, S. *M.U. J. Sci. Tech.,* **1986,** *3*, 195.
[26] Küçükgüzel, I.; Küçükgüzel, _.G.; Rollas, S.; Ötük-Sanı_, G.; Özdemir, O.; Bayrak, I.; Altu_, T.; Stables, J. P. *Farmaco*, **2004**, *59*, 893.
[27] Rollas, S.; Kalyoncuo_lu, N.; Sür-Altıner, D.; Ye_eno_lu, Y. *Pharmazie,* **1993**, *48*, 308.
[28] Küçükgüzel, I.; Rollas, S.; Çevikba_, A. *Drug Metab. Drug Interact*., **1995**, *12*, 151.
[29] Collins, L.; Franzblau, S.G. *Antimicrob. Agents Chemother.,* **1997**, *41*, 1004.
[30] Küçükgüzel, _.G.; Rollas, S.; Küçükgüzel, I.; Kiraz, M. *Eur. J. Med. Chem.,* **1999**, *34*, 1093.
[31] Tetko I.V.; Kovalishyn V.V.; Livingstone D. J. *J. Med. Chem.,* **2001**, *44,* 2411.
[32] Kohonen, T. *Self-organisation Maps*; Springer-Verlag: Berlin, **1995**.
[33] Tetko, I.V. *J. Chem. Inf. Comput. Sci.,* **2002**, *42*, 717.
[34] Virtual Computational Chemistry Laboratory (http://www.vcclab.org).
[35] Tetko, I.V.; Villa, A. E. P.; Livingstone, D. J. *J. Chem. Inf. Comput. Sci.,* **1996**, *36*, 794.
[36] Kovalishyn, V.V.; Tetko, I.V.; Luik, A. I.; Kholodovych, V. V.; Villa, A. E. P.; Livingstone, D.J. *J. Chem. Inf. Comput. Sci.,* **1998**, *38*, 651.
[37] Gilbert K.; Gaevski, J. *A MMPi Molecular Mechanics Program, Indiana University, Indiana,* **1985**.
[38] Dewar, M.J.S.; Zoebisch, E.G.; Healy E.F.; Stewart, J.J.P. *J. Am. Chem. Soc*., **1985**, *107*, 3902.
[39] Rollas, S.; Yılmaz, N.; Erdeniz, H.; Kiraz, M. *Med. Sci. Res.,* **1998**, *26*, 83.

Received: 21 November, 2005 **Revised: 05 April, 2006** **Accepted: 06 April, 2006**